Cardiovascular Research (2010) **87**, 73–82
doi:10.1093/cvr/cvq035

The histone deacetylase inhibitor suberoylanilide hydroxamic acid reduces cardiac arrhythmias in dystrophic mice

Claudia Colussi[1†], Roberta Berni[2†], Jessica Rosati[3], Stefania Straino[3], Serena Vitale[3], Francesco Spallotta[3], Silvana Baruffi[2], Leonardo Bocchi[2], Francesca Delucchi[2], Stefano Rossi[2], Monia Savi[2], Dante Rotili[4], Federico Quaini[2], Emilio Macchi[2], Donatella Stilli[2], Ezio Musso[2], Antonello Mai[4], Carlo Gaetano[3*], and Maurizio C. Capogrossi[3*]

[1]Laboratorio di Biologia Vascolare e Medicina Rigenerativa, Centro Cardiologico Monzino-IRCCS, Milano, Italy; [2]Interdepartmental Centre for the Study of Biology and Clinical Application of Cardiac Stem Cells (CISTAC), University of Parma, Parma, Italy; [3]Laboratorio di Patologia Vascolare, Istituto Dermopatico dell' Immacolata-IRCCS, Via Monti di Creta 104, Roma 167, Italy; and [4]Department of Pharmacological Science, University of Rome 'La Sapienza', Rome, Italy

Received 20 August 2009; revised 23 January 2010; accepted 26 January 2010; online publish-ahead-of-print 17 February 2010

Time for primary review: 19 days

Aims The effect of histone deacetylase inhibitors on dystrophic heart function is not established. To investigate this aspect, dystrophic mdx mice and wild-type (WT) animals were treated 90 days either with suberoylanilide hydroxamic acid (SAHA, 5 mg/kg/day) or with an equivalent amount of vehicle.

Methods and results The following parameters were evaluated: (i) number of ventricular arrhythmias in resting and stress conditions (restraint test) or after aconitine administration; (ii) cardiac excitability, conduction velocity, and refractoriness; (iii) expression and distribution of connexins (Cxs) and $Na_v1.5$ sodium channel. Ventricular arrhythmias were negligible in all resting animals. During restraint, however, an increase in the number of arrhythmias was detected in vehicle-treated mdx mice (mdx-V) when compared with SAHA-treated mdx (mdx-SAHA) mice or normal control (WT-V). Interestingly, aconitine, a sodium channel pharmacologic opener, induced ventricular arrhythmias in 83% of WT-V mice, 11% of mdx-V, and in 57% of mdx-SAHA. Epicardial multiple lead recording revealed a prolongation of the QRS complex in mdx-V mice in comparison to WT-V and WT-SAHA mice, paralleled by a significant reduction in impulse propagation velocity. These alterations were efficiently counteracted by SAHA. Molecular analyses revealed that in mdx mice, SAHA determined Cx remodelling of Cx40, Cx37 and Cx32, whereas expression levels of Cx43 and Cx45 were unaltered. Remarkably, Cx43 lateralization observed in mdx control animals was reversed by SAHA treatment which also re-induced $Na_v1.5$ expression.

Conclusion SAHA attenuates arrhythmias in mdx mice by a mechanism in which Cx remodelling and sodium channel re-expression could play an important role.

Keywords Arrhythmias • Ion channels • Connexins • Duchenne • Histone deacetylases

1. Introduction

Duchenne muscular dystrophy (DMD) is a genetic disease characterized by a progressive skeletal and cardiac muscle dysfunction determined by the absence of the structural protein dystrophin.[1] Recent clinical evaluation indicated that more than 30% of DMD deaths result from progressive deterioration of cardiac function and ensuing cardiac failure. Further, as fatal respiratory deficits are now treated with ventilatory assist devices, the cardiac involvement of Duchenne patients is emerging as a prevalent clinical feature and

† These authors contributed equally to this work.

* Corresponding author. Tel: +39 0666462429; fax: +39 0666462430, Email: capogrossi@idi.it, gaetano@idi.it

a major determinant of morbidity and mortality. Many DMD patients, in fact, develop dilated cardiomyopathy and heart failure. Electrocardiographic (ECG) abnormalities can be detected in up to 60% of the 10-year-old DMD population,[2] characterized by tall right precordial R-waves, decreased S:R ratio, and deep Q-waves.[2] Although in the early stages of the disease, the cardiac involvement remains subclinical with a normal echocardiographic pattern, with age and consequent fibrosis spreading left ventricular dysfunction and ventricular arrhythmias eventually occur.

Ventricular arrhythmia is a common complication in DMD patients and is considered a risk factor for sudden death.[3] The incidence of ventricular arrhythmias, in fact, increases with the progression of myocardial involvement and, although altered electrogenesis is not the most prevalent mechanism of dystrophic heart failure, severe arrhythmias frequently co-exist with asymptomatic left ventricular dysfunction and wall motion abnormalities thus contributing to sudden death. The pathogenesis of DMD is frequently studied in the dystrophic mdx mouse model. Although to a milder extent, the heart of these animals exhibits many of the most relevant features of DMD cardiomyopathy, showing progressive development of cardiac abnormalities including conduction defects, arrhythmias, and dilated cardiomyopathy. Although extensive accumulation of connective tissue and heart failure develop only in older mdx mice, electrical and molecular cardiac alterations can be detected at very early stages, suggesting that they may precede and contribute to the further development of the disease.

Recent studies reported that mutations in the SCN5 gene,[4] encoding for the sodium channel $Na_v1.5$, may cause dilated cardiomyopathy in humans, suggesting for a potential pathogenetic role of this molecule. This main voltage-gated sodium channel, in fact, plays a key role in cardiac conduction and its association with dystrophin C-terminus mediated by α and β syntrophins has been recently described.[4] The decreased $Na_v1.5$ protein level, associated with the global reduction of the dystrophin protein complex, is believed to be responsible for the lower sodium current present in mdx mice providing pathophysiological basis for at least some of the alteration observed in their hearts. Consistently, heterozygous SCN5A-knockout mice, a model for Lenègre's disease characterized by mutations in the $Na_v1.5$ channel, develop arrhythmias, extensive fibrosis, and changes in connexins (Cxs) expression, suggesting an association between the Na+ channel and gap junction proteins with potential pathogenetic relevance. Studies of Cx expression in diseased human and experimental animal hearts suggest that the altered expression or function of gap junctions often parallels arrhythmias occurring in many forms of heart disease, including hypertrophic, ischaemic, and dilated cardiomyopathies.[5] At present, no information is available on $Na_v1.5$ sodium channel expression or Cxs remodelling in the heart of DMD patients. Notably, the epigenetic regulatory enzymes histone deacetylases have been recently implicated in the pathogenesis of cardiac hypertrophy[6,7] and heart failure as well as in the process of skeletal muscle differentiation and regeneration including muscular dystrophy.[7–9] Alteration of their function has been associated with a number of clinical disorders including cancer, the chronic obstructive pulmonary disease, and neurodegenerative disorders. Although, the normalization of atrial arrhythmias and fibrosis, developing in a mouse model of cardiac hypertrophy, has been described following histone deacetylase inhibitors administration,[10] no information about their effect on the dystrophic heart is currently available. To address this clinically relevant issue, we analysed at electrophysiological (EP), structural, and molecular level, the heart of mdx mice treated with histone deacetylase inhibitors when compared with untreated mdx and normal control. Our results indicate the presence of ventricular arrhythmias detectable in mdx mice under stress condition which are reversed by histone deacetylase inhibitors. This effect is paralleled by sodium channel $Na_v1.5$ re-expression and Cx remodelling.

2. Methods

2.1 Animal population and treatment

Two-month-old mdx mice and syngeneic controls, strain C57/BlJ10 (Charles River), were used in all the experiments. Mice were injected ip daily either with the histone deacetylase inhibitor suberoylanilide hydroxamic acid (ALEXIS-Biochemicals) (SAHA 5 mg/kg body weight) or saline solution with an equivalent amount of solvent (DMSO). At this dosage, no effects beyond that of histone deacetylase inhibition are known or have been reported so far. Schedule and dosage of SAHA administration were derived from prior work.[9,11] All experimental procedures were approved by the internal Animal Research Ethical Committee (Protocol HH39) according to the Italian Ministry of Health and complied with the National Institutes of Health Guide for the Care and Use of Laboratory Animals (NIH publication No. 85-23, revised in 1996).

2.2 EP studies

2.2.1 Telemetry ECG recording

Wild type (WT) and 21 mdx mice daily injected with vehicle (WT-V, $n = 16$; mdx-V, $n = 21$; respectively) were studied in comparison to SAHA-treated WT and mdx animals (WT-SAHA, $n = 12$; mdx-SAHA, $n = 18$). All mice were chronically instrumented with a miniaturized telemetry ECG transmitter (model TA10ETA-F20, Data Sciences) to enable ECG recording in conscious freely moving animals, avoiding the confounding effects of anaesthesia according to a procedure described previously.[12] One week after surgery, continuous ECG recording was performed in baseline condition (15 min) and during manoeuvres (additional 15 min) aimed at inducing arrhythmias by stressful environmental conditions (restraint test: WT-V, $n = 10$; WT-SAHA, $n = 12$; mdx-V, $n = 11$; mdx-SAHA, $n = 11$)[13] or pharmacological treatment (aconitine administration, 5 mg/kg; WT-V, $n = 6$; mdx-V, $n = 9$; mdx-SAHA, $n = 7$).[14] In brief, restraint test consisted of introducing the experimental animal in a plexiglass tube (internal diameter, 3 cm; length, 10 cm), closed at both ends by removable partitions provided with holes. All experimental sessions were performed in a daylight interval between 10.00 a.m. and 1.00 p.m. Telemetry ECGs were collected by a receiver (model CTR85-SA, Data Sciences) placed under the experimental cage. Data were A-D converted, stored on computer memory, analysed off-line in order to detect cardiac rhythm disturbances, and determine heart rate and heart rate-based indices of cardiac autonomic input.

These indices included the standard deviation of R–R interval (SD_{RR}) and the square root of the mean of the squared differences between adjacent R–R interval (r-MSSD), taken, respectively, as indices of cardiac sympathovagal balance and vagal input to the heart.

2.2.2 Epicardial multiple lead recording

Additional WT-V ($n = 4$), WT-SAHA ($n = 3$), mdx-V ($n = 3$), and mdx-SAHA ($n = 4$) were subjected to cardiac EP testing by using a 5 × 5 row and column electrode array with a 0.6 mm resolution square mesh. Epicardial unipolar electrograms (EGs) were recorded during sinus rhythm or specific pacing protocols in order to determine: (i) epicardial conduction velocity (CV), (ii) cardiac excitability and refractoriness, respectively, by strength–duration curve (*S–D* curve) and effective refractory period (ERP) measurements, and (iii) duration of QRS, QT, and

corrected QT interval (QTc) measured from the root mean square (RMS) signal computed from all of the 5 × 5 EGs.

Further methodological information are available in the Supplementary material online section.

2.3 Antibodies and western blotting

Western blotting (WB) analysis was performed according to standard procedure. Heart samples were lyzed in Laemli's buffer plus protease and phosphatase inhibitor mix (Sigma).

Results of WB were analysed by ImageJ v1.28 software. Optical density values of specific proteins were normalized to those of tubulin and corrected for those obtained from WT which were considered equal to 1. Data represent the mean of at least three independent experiments ± standard error of the mean. The following antibodies were used for either WB or immunofluorescence (IF) analysis: anti-Cx40, -Cx45, and -Cx37 (WB 1:250, polyclonal; Zymed); anti-Cx43 (WB 1:8000; IF 1:100, polyclonal; Abcam); and anti-Cx32 (WB 1:1000, polyclonal; Abcam); anti α-tubulin (WB 1:4000, monoclonal; Sigma); anti-$Na_v1.5$ (IF 1:100, polyclonal; Abcam) (WB 1:2000; IF 1:100, polyclonal; Aviva); and anti-dystrophin (WB 1:200, polyclonal; Abcam).

2.4 Confocal analysis

Heart sections were deparaffinized and confocal IF analysis performed according to a procedure described previously.[8] Briefly, sections were incubated for 1 h with 10% BSA/PBS to block non-specific protein-binding sites and overnight at 4°C with specific antibodies. After a brief rinse, sections were incubated with FITC or TRITC secondary antibodies (dilution 1:50, DAKO). Nuclei were counterstained with TOPRO3. Samples were analysed using a Zeiss LSM510 Meta Confocal Microscope with ×40 or ×120 magnification. Lasers' power, beam splitters, filter settings, pinhole diameters, and scan mode were the same for all examined fields of each sample. Negative IF control was performed using normal rabbit IgG instead of the rabbit primary antibody.

2.5 Proteasome activity

Proteasome activity was measured on 100 μg of whole hearts lysates according to manufacturer's instructions (20S proteasome activity assay, Chemicon).

Tissues have been homogenized in lysis buffer containing 50 mM HEPES (pH 7.5), 5 mM EDTA, 150 mM NaCl, and 1% Triton X-100.

2.6 Statistical analysis

The SPSS statistical package was used (SPSS, 15th version). Normal distribution of variables was checked by means of the Kolmogorov–Smirnov test. Statistics of variables normally distributed (all variables except baseline arrhythmias) included mean ± standard error (SE), two-tailed Student's *t*-test, one-way analysis of variance (*post hoc* analysis: Bonferroni or Games–Howell test, when appropriate), and χ^2 test. Non-parametric statistical tests (Kruskal—Wallis test and Mann–Whitney *U*-test) were used to evaluate differences in the incidence of baseline ventricular arrhythmias among groups and differences between baseline and stress-induced arrhythmias within each group. Statistical significance was set at $P < 0.05$.

3. Results

3.1 SAHA exerts anti-arrhythmic properties in mdx mice

3.1.1 Telemetry ECG recording

Experiments were performed to establish the effect of SAHA on electrogenesis and autonomic modulation of the dystrophic heart, in conscious and freely moving mice.

3.1.1.1 Baseline conditions

In all groups, spontaneous ventricular arrhythmias, consisting of isolated premature beats, were negligible (WT-V, 0.9 ± 0.2 events; WT-SAHA, 0.5 ± 0.2; mdx-V, 1.7 ± 0.4; mdx-SAHA, 1.2 ± 0.5), and the average values of R–R interval, SD_{RR}, and r-MSSD were comparable (*Table 1*).

3.1.1.2 Restraint test

In this condition, the exposure to stress significantly decreased R–R interval (−20%; $P < 0.01$) and heart rate variability indices (SD_{RR}, −80%; r-MSSD, −70%; $P < 0.01$, *Table 1*) in all the animals tested. Conversely, significant differences among groups were found in the number of stress-induced ventricular arrhythmias.

In comparison to WT animals treated with vehicle alone or SAHA, control mdx exhibited a significant increase ($P < 0.05$) in the number and complexity of arrhythmias including isolated premature ventricular beats (PVBs), several salvos, and short episodes of ventricular tachycardia. Although only nine out of 141 ventricular arrhythmic episodes documented during restraint test in the entire animal population consisted of ventricular tachycardia, all of them occurred in mdx-V mice (*Table 2* and *Figure 1*, see also Supplementary material online).

The restraint test activates arrhythmogenic pathways via sympathetic over-stimulation,[13] leading to increased dishomogeneity of

Table 1 Heart rate and heart rate variability indices (telemetry ECG data)

	WT-V ($n = 10$)	WT-SAHA ($n = 12$)	mdx-V ($n = 12$)	mdx-SAHA ($n = 11$)
Baseline				
R–R (ms)	108 ± 5	129 ± 8	116 ± 6	117 ± 7
SD_{RR} (ms)	12.7 ± 2.3	17.3 ± 2.3	10.7 ± 1.3	11.6 ± 1.1
r-MSSD (ms)	4.3 ± 1.1	5.5 ± 1.0	5.6 ± 1.2	3.2 ± 0.6
Restraint				
R–R (ms)	86 ± 1*	85 ± 1*	88 ± 2*	87 ± 2*
SD_{RR} (ms)	1.5 ± 0.1*	1.9 ± 0.1*	1.8 ± 0.1*	1.7 ± 0.1*
r-MSSD (ms)	1.0 ± 0.02*	1.1 ± 0.01*	1.2 ± 0.06*	1.1 ± 0.03*

Heart rate and heart rate variability indices in WT-V, WT-SAHA, mdx-V, and mdx-SAHA mice, in baseline and during restraint test. Values are expressed as mean ± SE.
*$P < 0.01$, significant differences vs. baseline values in each experimental group.

Table 2 Ventricular arrhythmias during restraint

	WT-V ($n = 10$)	WT-SAHA ($n = 12$)	mdx-V ($n = 12$)	mdx-SAHA ($n = 11$)
Mean ± SE	0.7 ± 0.2	1.2 ± 0.5	9.7 ± 3.5*,#	1.2 ± 0.5
Types of arrhythmias				
PVBs (range)	(1–3) in 6 mice	(1–5) in 5 mice	(1–27) in 11 mice	(1–5) in 6 mice
Salvos	None	None	(1–7) in 4 mice	1 in one mice
VT	None	None	(2–5) in 3 mice	None
No. of animals without arrhythmias	4 out of 10	7 out of 12	None	4 out of 11

Analysis of ventricular arrhythmic events during restraint in WT-V, WT-SAHA, mdx-V, and mdx-SAHA mice. PVBs, premature ventricular beats; Salvo, run of two or three consecutive PVBs; VT, ventricular tachycardia (run of four or more consecutive PVBs).
*$P < 0.05$ significant differences vs. WT-V and WT-SAHA.
#$P < 0.05$ significant differences vs. mdx-SAHA.

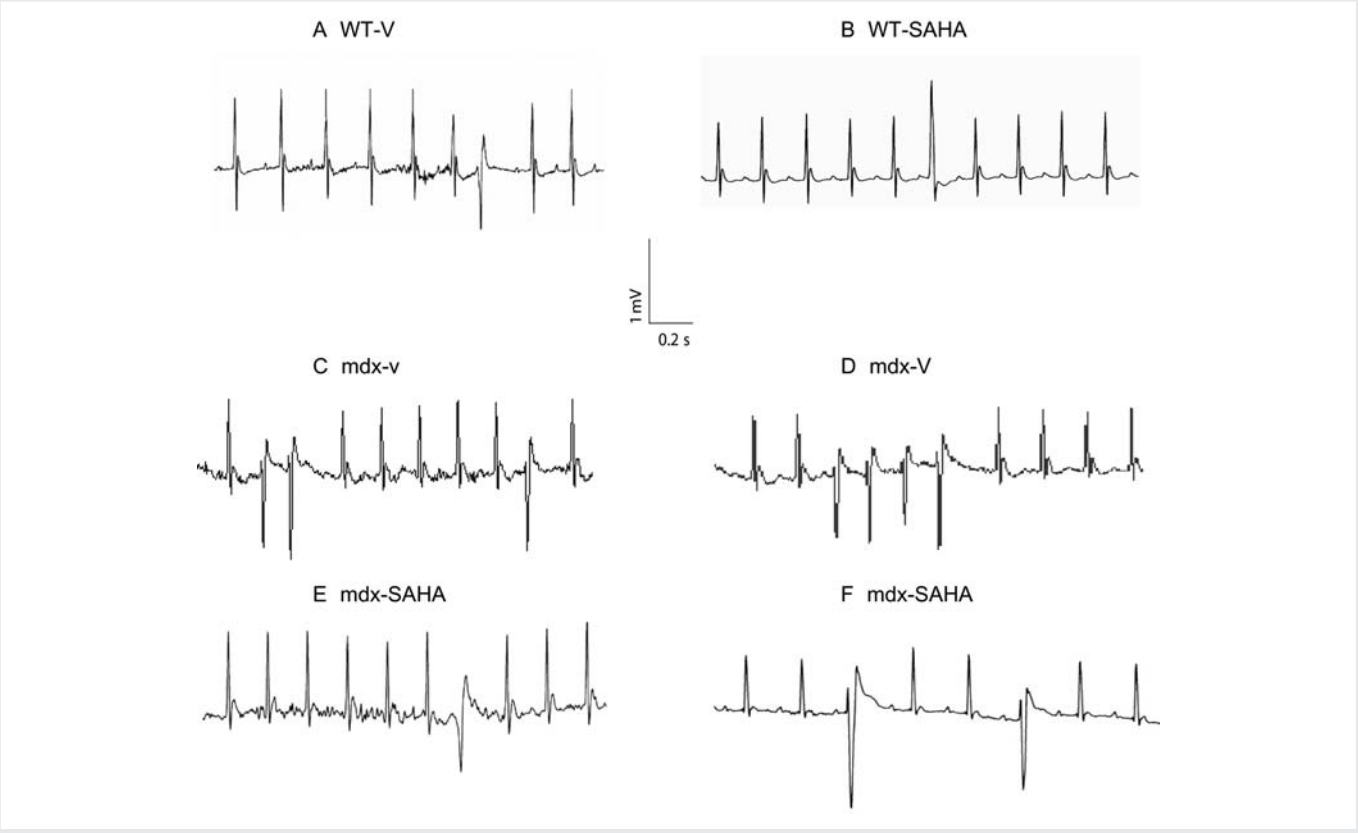

Figure 1 Telemetry ECG tracings. Representative telemetry ECGs illustrating different patterns of ventricular arrhythmias during restraint in WT-V, WT-SAHA, mdx-V, and mdx-SAHA mice. (*A*, *B*, *E* and *F*) Isolated PVBs. (*C*) One salvo and one PVB. (*D*) A short episode of ventricular tachycardia.

repolarization and abnormal impulse initiation as a consequence of increased local potential gradients or afterdepolarizations.[15] The higher electrical instability observed in control mdx could, therefore, be a consequence of arrhythmogenic mechanisms triggered by increased sympathetic activity. Remarkably, in the mdx-SAHA group, the occurrence and severity of arrhythmias were drastically reduced ($P < 0.05$ vs. mdx-V), indicating a protective role for this treatment against ventricular electrical instability (*Table 2* and *Figure 1*). Further, the lack of significant differences in SD_{RR} and r-MSSD (*Table 1*) suggests that the anti-arrhythmic action of SAHA is not mediated by changes in cardiac autonomic modulation but rather results from a direct effect on myocardial tissue.

3.1.1.3 Aconitine administration

To investigate whether the positive effect of SAHA on cardiac electrical competence implies a reconstitution of the $Na_v1.5$ sodium channel function, we analysed arrhythmias in the presence of aconitine, a pro-arrhythmic drug known to maintain the sodium channel in an open state. In this condition, high incidence of isolated PVBs and several episodes of ventricular tachycardia occurred in WT-V mice

(83%). Interestingly, the severity of aconitine-dependent arrhythmias was limited to isolated premature beats in both mdx-V and mdx-SAHA mice, whereas the percentage of animals exhibiting arrhythmias was significantly reduced in the control mdx-V group (11%, $P < 0.05$) but not in mdx-SAHA (57%) (*Table 3*). Thus, our data might reflect a reduced level of Na^+ channels, the aconitine arrhythmogenic substrate, observed in untreated mdx mice,[4] which is reverted by SAHA (*Table 3*).

3.1.2 Epicardial multiple lead recording

To further investigate ventricular electrogenesis in WT-V, WT-SAHA, mdx-V, and mdx-SAHA mice, we performed high-resolution epicardial recordings in order to determine the EP properties of the normal vs. dystrophic myocardial tissue, including excitability, CV, and refractoriness. Of note, the appropriate positioning of the electrode array was in some cases prevented by an unfavourable spatial relationship between heart and lungs during the open chest preparation. In addition, in a limited number of animals, the light pressure exerted by the electrode injured the delicate and thin visceral pericardium. Both conditions determined that only a fraction of the 25 epicardial sites explored by the electrode grid or used for pacing (five selected electrodes, see Supplementary material online, *Figure S1F*) were excitable and/or enabled recording of reliable EG signals.

Table 3 Animals exhibiting ventricular arrhythmias following aconitine administration

	WT-V ($n = 6$)	mdx-V ($n = 9$)	mdx-SAHA ($n = 7$)
Animals with arrhythmias	5 (83%)	1 (11%)	4 (57%)
Animals without arrhythmias	1 (17%)	8 (89%)	3 (43%)
		*	n.s.

Animals exhibiting ventricular arrhythmic events following aconitine administration in WT-V, mdx-V and mdx-SAHA. n.s. indicates no statistically significant differences between mdx-SAHA and WT-V.
*Differences between mdx-V and WT-V are statistically significant ($P < 0.05$).

3.1.2.1 EG interval duration

The duration of QRS, QT, and QTc intervals was determined by means of RMS curves obtained from 90, 66, 61, and 93 beats recorded in WT-V, WT-SAHA, mdx-V, and mdx-SAHA mice, respectively (*Table 4*). QRS duration was increased by about 30% in mdx-V mice compared with WT-V and WT-SAHA animals ($P < 0.01$), whereas the prolongation was partially reduced in SAHA-treated mdx mice (*Table 4*). QT and QTc intervals did not exhibit any difference among groups (*Table 4*). Unlike measurements performed in conscious animals, the average values of R–R interval under anaesthesia were significantly higher in WT-SAHA and mdx-V mice. However, similar values of QRS were obtained during periods of comparable heart rate in each group, thus excluding any effects of different R–R values on QRS duration (*Table 4*).

3.1.2.2 Excitability

S–D curves 9, 4, 6, and 7 could be correctly determined in WT-V, WT-SAHA, mdx-V, and mdx-SAHA animals, respectively, and an equivalent number of rheobase (Rh) and chronaxie (Chr) values were analysed. In mdx-V mice, *S–D* curves were shifted upward and to the right resulting in about two-fold increase in Rh when compared with the other groups ($P < 0.01$; *Figure 2A*). A similar tendency was observed for Chr values (*Figure 2B*).

3.1.2.3 Conduction velocity

CV was analysed longitudinally (CV-l) and transversally (CV-t) to fibres orientation at the 27 and 24 epicardial sites in WT-V mice, the 12 and 15 sites in WT-SAHA, the 58 and 49 sites in mdx-V, and the 44 and 51 sites in mdx-SAHA. Both values were significantly lower in mdx-V mice compared with WT-V and WT-SAHA (−30 and −15%, respectively, $P < 0.01$). Notably, the SAHA treatment reverted CV-t to WT level, whereas it was ineffective on CV-l (*Figure 2C* and *D*).

3.1.2.4 Refractoriness

The ERP was measured at the 9, 7, 12, and 11 epicardial sites in WT-V, WT-SAHA, mdx-V, and mdx-SAHA animals. ERP was about 37% longer in mdx-V mice when compared with both WT-V and WT-SAHA groups ($P < 0.01$). This prolongation was abolished by SAHA treatment (*Figure 2E*).

Taken altogether, these EP data indicate a deterioration of ventricular excitatory processes in mdx-V animals, as revealed by (i) QRS

Table 4 R–R, QRS, QT, and QTc interval duration

	WT-V	WT-SAHA	mdx-V	mdx-SAHA
Animals (no. of beats)	4 (90)	3 (66)	3 (61)	4 (93)
QRS (ms)	11.5 ± 0.7	11.7 ± 0.5	15.4 ± 0.5*,§	14.1 ± 0.5
QT (ms)	23.3 ± 0.6	20.2 ± 1.5	29.7 ± 5.3	26.4 ± 2.9
QTc (ms)	16.9 ± 0.9	11.5 ± 0.6	16.9 ± 3.7	15.9 ± 1.4
R–R (ms)	209 ± 7	308 ± 18*	327 ± 29*	267 ± 24
QRS (ms) comparable R–R (ms)	11.8 ± 0.2 (227 ± 0.4)	10.3 ± 0.2 (277 ± 2.3)	16.7 ± 0.3 (257 ± 2.0)	14.7 ± 0.2 (220 ± 0.9)

Measurements of QRS, QT, and QTc interval duration in WT-V, WT-SAHA, mdx-V, and mdx-SAHA mice. QRS, duration of QRS complex; QT, duration of QT interval; QTc, QT interval normalized to cycle length.
*$P < 0.05$ significant differences vs. WT-V.
§$P < 0.05$ significant differences vs. WT-SAHA.

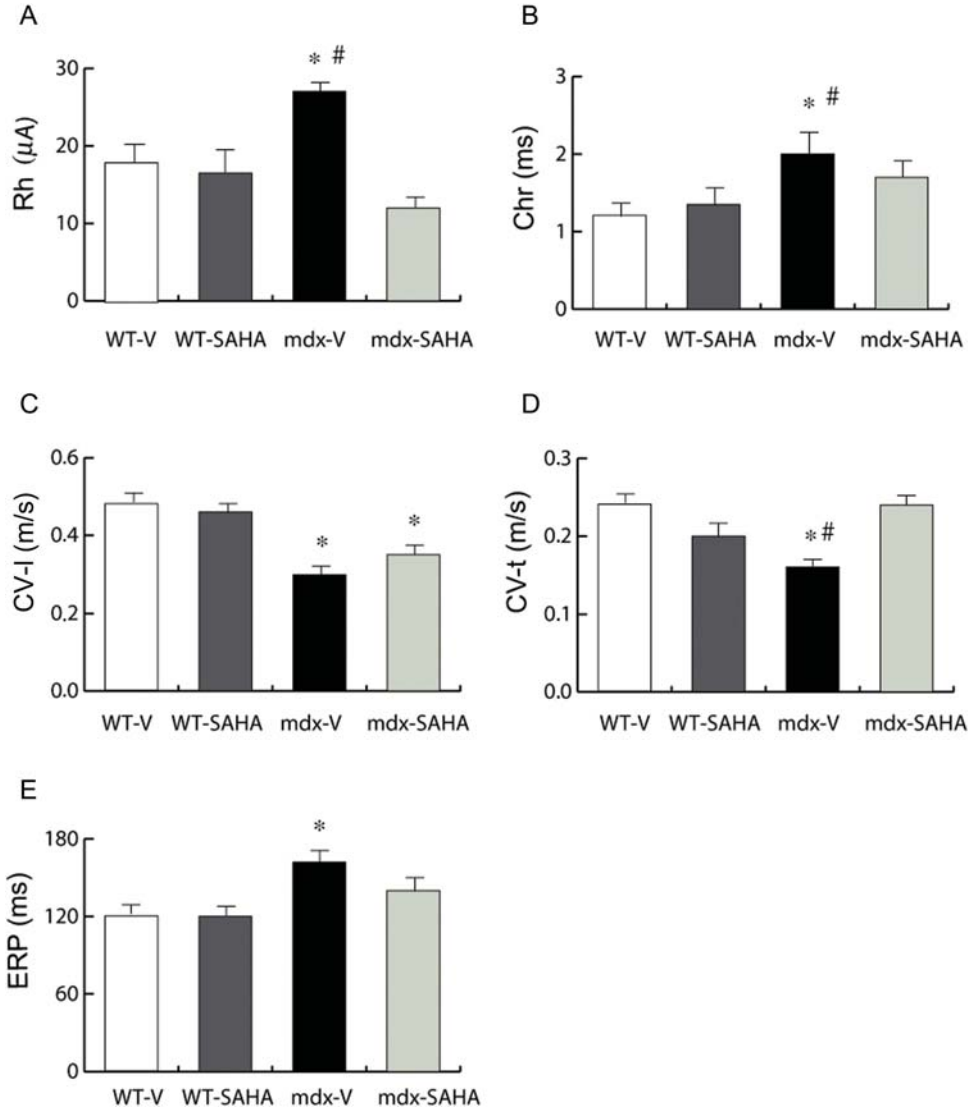

Figure 2 Cardiac excitability, CV, and refractory period in WT groups, mdx-V, and SAHA-treated mdx mice. Average values ± SE of (*A*) Rh, (*B*) Chr, (*C* and *D*) CV measured longitudinally (CV-l) and transversally (CV-t) to myocardial fibre orientation, and (*E*) duration of the ERP. *$P < 0.01$ significant differences vs. WT-V and WT-SAHA; #$P < 0.01$ significant differences between mdx-V and mdx-SAHA groups.

prolongation, (ii) slow-down of excitation spreading and decrease in CV, and (iii) reduced ability to elicit a propagated response as a consequence of reduced excitability and increased refractoriness. These alterations were largely reversed by SAHA treatment. Interestingly, these changes were apparently independent on connective tissue accumulation as demonstrated by the presence of similar levels of hydroxyproline content in WT-V, mdx-V, and mdx-SAHA mice (WT-V = 0.118 ± 0.02, mdx-V = 0.13 ± 0.021, and mdx-SAHA = 0.115 ± 0.03 μg hydroxyproline/mg tissue; $n = 6$ in each group).

3.2 SAHA induces Cx remodelling and modulates expression and function of the $Na_v1.5$ sodium channel

In this study, we describe the amelioration of cardiac electrical competence in SAHA-treated mdx mice paralleled by an improvement of the electrical impulse propagation throughout the myocardium. We reasoned that this effect could rely on active and passive recovery of the electrical properties of the heart. In fact, the type and distribution of gap junctions and the Na^+ ions current, responsible for the initial phase of the action potential and delivering of local current to propagation,[16] are generally admitted as the main determinants of the cardiac conduction. Therefore, we investigated the involvement of Cxs and the cardiac voltage-gated sodium channel $Na_v1.5$ isoform in determining the effects of SAHA on cardiac electrogenesis.

3.2.1 Cx remodelling

The expression of cardiac (Cx40, Cx43, and Cx45) and non-cardiac specific Cxs (Cx37 and Cx32) was evaluated. WB analysis performed on whole heart lysates obtained from WT-V and mdx-V mice showed comparable Cx43 and Cx45 protein levels. In contrast, Cx40 was found up-regulated in mdx-V mice (*Figure 3A*). Remarkably, the

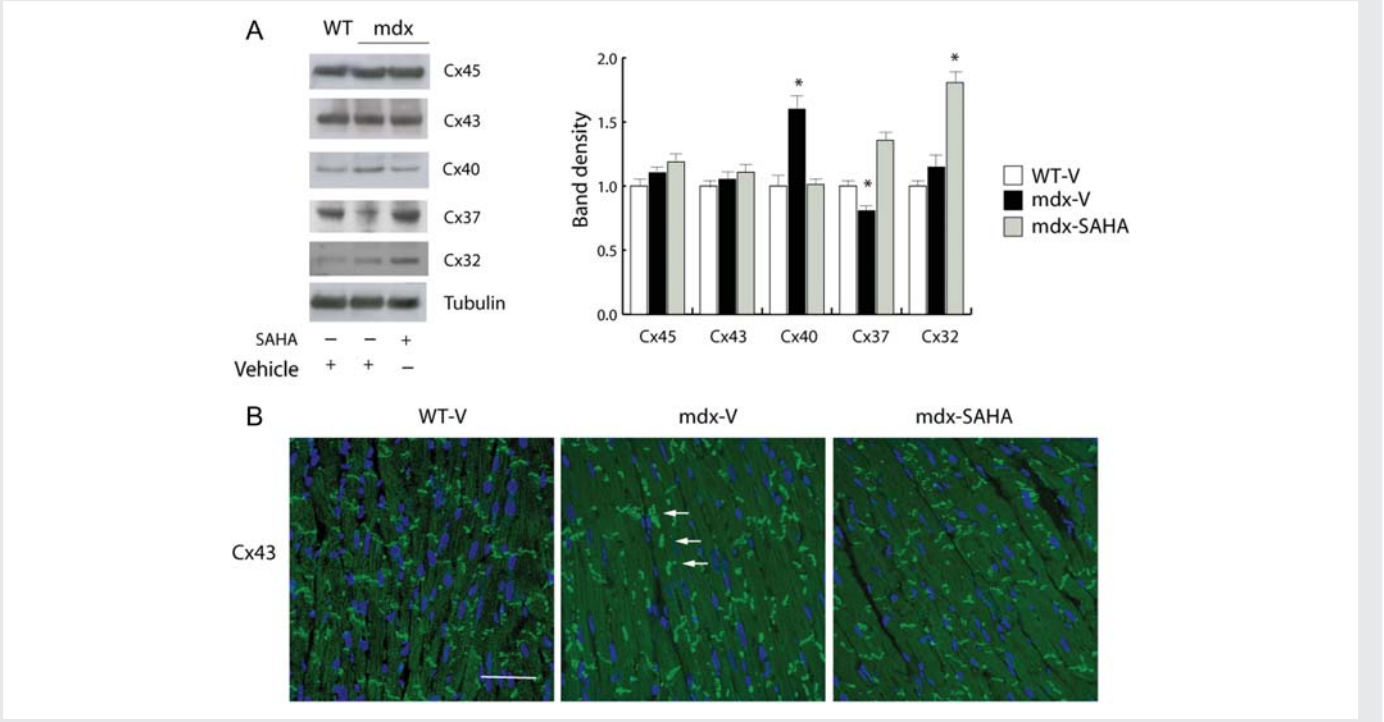

Figure 3 Cx remodelling induced by SAHA treatment. (*A*) WB evaluation of Cx43, Cx40, Cx45, Cx32, and Cx37 protein levels (left panel) and densitometric analysis (right panel). (*B*) Representative confocal analysis image of Cx43 distribution in the ventricular myocardium of WT-V, mdx-V and mdx-SAHA mice; nuclei were counterstained with TOPRO3 (scale bar 50 μm) ($n = 3$). Arrows indicate the presence of lateralized Cx43 on mdx cardiomyocytes. *$P < 0.05$ significant differences vs. WT-V.

normal distribution of Cx43 in the gap junctions at the apical cell-to-cell contacts was lost in mdx-V heart where a marked Cx43 lateralization was observed (*Figure 3B*). This finding is in agreement with what observed in other types of cardiac dysfunction. In failing heart, in fact, a loss of the normal ordered distribution of Cx43 is often evident at the border zone close to the scar tissue,[17] whereas an increase in Cx40 level has been observed in patients with congestive heart failure secondary to dilated cardiomyopathy.[18] Remarkably, SAHA treatment modified the pathological pattern of Cxs of mdx mice; it decreased the protein level of Cx40 (*Figure 3A*) and significantly recovered to a normal Cx43 distribution pattern (*Figure 3B*). No changes in Cx43 distribution were observed in WT-SAHA group (see Supplementary material online, *Figure S3*). The non-cardiac specific Cxs Cx32, expressed by cardiac fibroblasts, and Cx37, present on endothelial cells, were also analysed. Although Cx37 was found down-regulated in mdx-V mice ($P < 0.05$), both molecules were significantly up-regulated in response to SAHA (*Figure 4A*). Altogether, these data indicate an important and generalized effect of SAHA on Cx expression and distribution in the dystrophic mouse heart.

In this study, data provided by epicardial recordings indicated that SAHA greatly improved excitability, refractoriness, and CV across fibres (CV-t) but failed to restore the altered spread of excitation along fibres (CV-l). This observation supports the hypothesis that gap junctions remodelling can contribute to the SAHA-dependent benefit to mdx cardiac electrical competence, but further suggests that other mechanisms could be involved in this process.

3.2.2 Modulation of function and expression of $Na_v1.5$ sodium channel isoform

The cardiac $Na_v1.5$ channels are localized at the intercalated disk region of cardiomyocytes as well as in the lateral membranes. Interestingly, dystrophin has been shown to be absent from the intercalated discs of normal human and murine cardiac cells. One of the consequences of dystrophin deficiency, in fact, is the down-modulation of the sodium channel $Na_v1.5$ which results in reduction of maximum Na^+ conductance and may play a role in arrhythmogenesis by decreasing velocity of impulse propagation and safety factor for conduction.[19] In addition, the results of our analysis about proneness to arrhythmias in WT-V, mdx-V, and mdx-SAHA mice challenged with aconitine suggest that part of the positive effect of SAHA on cardiac conduction may reflect the reconstitution of the sodium channel $Na_v1.5$ function. In order to investigate this aspect, WB (*Figure 4A*, left panel) analyses of hearts from control or SAHA-treated animals were performed. The result shows that SAHA induced $Na_v1.5$ channel re-expression. Confocal microscopy performed with two different antibodies raised against the $Na_v1.5$ sodium channel (*Figure 4B* and see Supplementary material online, *Figure S2*) confirmed this result.

The sodium channel $Na_v1.5$ association with the dystrophin C-terminal is believed responsible for the channel protein stabilization. In an independent series of experiments, we evaluated whether the $Na_v1.5$ re-expression could be associated to dystrophin re-expression. Similar to what previously observed in the skeletal muscle of mdx mice treated with histone deacetylase inhibitors,[9] SAHA did not induced dystrophin expression in mdx heart (*Figure 4A*, right panel), re-enforcing

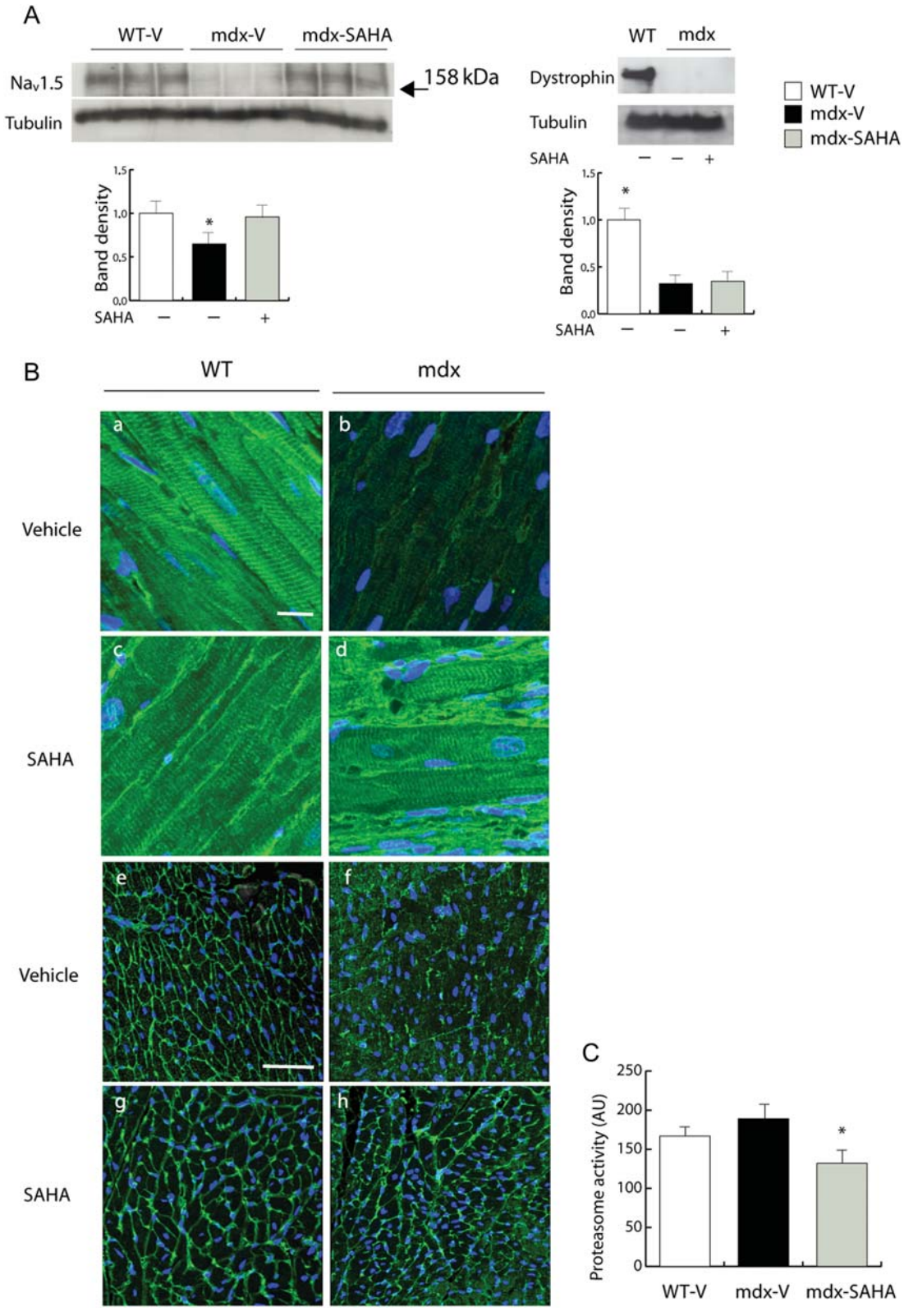

Figure 4 Evaluation of expression of the sodium channel $Na_v1.5$. (*A*) Evaluation of $Na_v1.5$ (left panel) or dystrophin (right panel) expression in WT-V, mdx-V and mdx-SAHA mice ($n = 3$). The graphs show the relative densitometric analysis. (*B*) Representative pictures showing $Na_v1.5$ expression in longitudinally (*a*–*d*) or transversally (e–*h*) oriented cardiac fibres by confocal analysis in WT-V (*a* and e), mdx-V (*b* and *f*), mdx-SAHA (*d* and *h*), and WT-SAHA (*c* and *g*) mice (scale bar: *a*–*d*, 10 μm; e–*h*, 50 μm) ($n = 3$). (*C*) Analysis of proteasome activity in whole heart lysates from WT-V, mdx-V, and mdx-SAHA mice (*$P < 0.05$).

the evidence that histone deacetylase inhibitors do not correct the primary genetic defect of DMD.

Several ions channels[20] including the cardiac $Na_v1.5$ have been shown regulated by ubiquitination. Specifically, van Bemmelen *et al.*[21] demonstrated that Nedd4-2 ubiquitinates $Na_v1.5$ modulating the intracellular pool of channels, possibly through proteasome-mediated cytosolic protein degradation. In this view, we investigated whether SAHA treatment could affect proteasome activity in mdx heart samples. *Figure 4C* shows that proteasome activity was slightly increased in mdx-V heart in comparison to WT-V and completely abrogated by SAHA treatment.

4. Discussion

Published data about cardiac electrical competence in mdx mice disclose a variety of contrasting observations possibly generated by a mix of heterogeneous variables including animal age, ECG acquisition techniques (i.e. standard ECG, Holter monitoring, and epicardial/intracardiac EP testing), recording conditions (i.e. conscious vs. anaesthetized animals), and genetic background.

In our experimental setting, we analysed arrhythmia vulnerability in conscious animals in order to detect early signs of cardiac electrical dysfunction. Ventricular arrhythmias were negligible in baseline condition in all the animals tested. In contrast, restraint conditions resulted in a significantly larger number of ventricular arrhythmias in mdx-V mice in comparison to control groups (WT-V and WT-SAHA), revealing a latent cardiac pathological state. One advantage of telemetry ECG recording during restraint for exploring the competence of cardiac electrical function is the use of stimuli belonging to the real life of social animals. On the other hand, the mouse high heart rate and the limitation of one-lead recording require a careful analysis of ECG signals and in some cases might make it difficult a clear cut interpretation. Thus, it is not excluded that additional important information on the electrical instability of mdx heart can be provided by more invasive EP studies with stress protocols. The occurrence of restraint-induced ventricular arrhythmias was reverted to control values in mdx-SAHA mice indicating a protective effect of the treatment. Notably, heart rate-based indices of autonomic input to the heart had similar values in all groups during both baseline and restraint, excluding any major involvement of cardiac autonomic modulation in mdx cardiomyopathy and in the mechanism of SAHA-dependent recovery. The percentage of animals with aconitine-induced ventricular electrical instability was significantly less in mdx-V group mice, when compared with the other groups, suggesting a role of Na^+ channel in the anti-arrhythmic effect of SAHA. Consistently, epicardial multiple lead recording in anaesthetized animals revealed: (i) longer QRS complex in mdx-V mice than in the control groups; (ii) decreased CV along and across fibres, and (iii) reduction in the ability to elicit a propagated response resulting from decreased excitability and increased refractoriness. Most of the degeneration in EP properties of the ventricular myocardium was largely counteracted by SAHA which, however, was unable to ameliorate CV along fibres. The significant prolongation of R–R interval as measured at the epicardial surface of anaesthetized WT-SAHA together with the observation that values of both R–R interval and SD_{RR} in conscious WT-SAHA mice tended to be higher than in control mice (WT-V) might suggest a slight facilitatory action of SAHA on the vagal input to the heart. This effect, however, is modest and should not have had any consequence on the SAHA-induced recovery of ventricular electrical stability in mdx mice. On the other hand, a longer R–R interval under anaesthesia was also observed in the control mdx-V group. Therefore, non-specific effects of anaesthesia cannot be completely ruled out at least for this parameter.

Structural remodelling of gap junctions involving abnormalities in the expression and distribution of Cxs has been found in different human heart diseases developing arrhythmias. Specifically, an altered distribution of Cx43 and Cx40 has been observed in patients with congestive heart failure secondary to dilated cardiomyopathy.[22] In our study, we found that alteration in Cx40 expression and in the spatial distribution of ventricular Cx43 occurred in mdx heart. Analysis of the epicardial CV revealed a slower impulse propagation both along (CV-l) and across (CV-t) mdx cardiac fibres when compared with controls. These results are compatible with alteration of Cx function consequent to lateralization or dysregulated expression level. Nevertheless, the treatment with SAHA reduced the expression of Cx40 and partially normalized the distribution of Cx43. Further, in mdx-V mice, the altered expression of Cx32, characteristic of cardiac fibroblast, and Cx37 expressed by endothelial cells were reverted to control values by SAHA treatment. Although the contribution of Cx37 and Cx32 to the development of arrhythmias is currently unclear, it is conceivable that the restoration of normal Cx levels may contribute to the functional normalization dystrophic cardiomyocytes. SAHA treatment, however, was not able to completely re-establish the normal CV-l values in mdx-SAHA group as indicated by epicardial EP testing.

The structural and functional interactions between cardiomyocytes and other cells, (e.g. cardiac fibroblast) are essential for heart physiology and pathophysiology.[23] Yet, despite the alteration in the level and/or spatial distribution of Cxs is important for cardiac impulse propagation and plays a role in arrhythmias development, further experiments are required in order to clarify (i) the exact contribution of Cxs remodelling to the development of cardiac arrhythmias in mdx mice, (ii) whether the dystrophin defect plays a role in this process, and (iii) how SAHA-dependent mechanisms contribute to Cxs normalization. In this context, the acetylation of specific target proteins elicited by SAHA and other inhibitors could be an important aspect to evaluate in future investigations.

Although the precise localization of the sodium channel $Na_v1.5$ in cardiac cells is somewhat controversial,[24] it is recognized that at least two distinct pools of $Na_v1.5$ channel may co-exist. One resides at the intercalated disks, whereas the other seems localized in lateral membranes, and recent findings raised the issue that this second pool of sodium channel could play an important role in the conduction of cardiac impulse.[25] In the heart, dystrophin and the sodium channel $Na_v1.5$ largely co-localize, at the peripheral plasma membrane and in the T-tubule system. On the other hand, differently from the sodium channel, dystrophin is absent from the intercalated discs of human and murine cardiomyocytes.[26] As a consequence of dystrophin mutation, an alteration in expression and function of the sodium channel $Na_v1.5$ has been recently described in mdx heart.[4] Our experiments showed that the treatment with SAHA led to the re-expression of this channel with important functional consequences as indicated by the re-establishment of proneness to aconitine-induced arrhythmias in SAHA-treated mdx. In addition, the epicardial EP recordings suggests that the amelioration of impulse propagation occurs predominantly across fibres, indicating that SAHA, although ineffective on the endogenous dystrophin levels, has an impact on $Na_v1.5$ channels including those present in

the lateral membranes and normally associated with dystrophin. The mechanism leading to $Na_v1.5$ alteration in mdx mice is not known. A physical link between dystrophin and this ion channel has been proposed to contribute to protein stability. Indeed, the increase in sodium channel protein level elicited by SAHA may underline the presence of still uncovered regulatory mechanisms. In fact, $Na_v1.5$ is known to associate with several proteins which may regulate the anchoring and clustering of the channel itself to the membrane even in the absence of dystrophin.[27–29] Further, ubiquitination is known to regulate the $Na_v1.5$ channel membrane density possibly targeting the protein for proteasome-mediated degradation.[21] The ability of SAHA to inhibit proteasome activity in mdx heart strongly suggests that this could be an important part of the mechanism responsible for the sodium channel re-expression. Further experiments are required to address this important aspect.

This is the first report about a histone deacetylase inhibitor which prevents ventricular arrhythmias and reverses conduction defects in the mouse dystrophic heart. This anti-arrhythmogenic action of SAHA occurs in the absence of effects on cardiac fibrosis which, at this stage of the disease, is similar in normal and dystrophic mice. Remarkably, SAHA normalized Cx40, reversed Cx43 lateralization, and re-induced $Na_v1.5$ expression, indicating, for this small molecule, novel properties potentially useful to reduce or prevent arrhythmogenesis and ventricular electrical dysfunction in DMD. Hence, our results indicate that histone deacetylase inhibitors and, more broadly, epigenetic drugs may represent a novel class of anti-arrhythmic agents awaiting development for clinical use.

Supplementary material

Supplementary material is available at *Cardiovascular Research* online.

Acknowledgement

C.C. is a PhD student at the 'Scienze Endocrino-Metaboliche ed Endocrino-Chirurgiche' School of the Chair of Endocrinology, Catholic University, Rome, Italy.

Funding

Research was partially supported by: FIRB grant # RBLA035A4X-1-FIRB to M.C.C., UE FP6 grant # UE-LHSB-CT-04-502988 to M.C.C., AFM grant # MNM2-06 to C.G. and # DdT2-06 to M.C.C., and MDA grant # 88202 to C.G. RB and MS are financially supported by "Compagnia di San Paolo".

Conflict of interest: none declared.

References

1. Engel AG, Yamamoto M, Fischback KH. *Dystrophinopathies*. 2nd ed. New York: McGraw-Hill; 1994.
2. Finsterer J, Stollberger C. The heart in human dystrophinopathies. *Cardiology* 2003;**99**:1–19.
3. Yanagisawa A, Miyagawa M, Yotsukura M, Tsuya T, Shirato C, Ishihara T *et al*. The prevalence and prognostic significance of arrhythmias in Duchenne type muscular dystrophy. *Am Heart J* 1992;**124**:1244–1250.
4. Gavillet B, Rougier JS, Domenighetti AA, Behar R, Boixel C, Ruchat P *et al*. Cardiac sodium channel Nav1.5 is regulated by a multiprotein complex composed of syntrophins and dystrophin. *Circ Res* 2006;**99**:407–414.
5. Gutstein DE, Morley GE, Tamaddon H, Vaidya D, Schneider MD, Chen J *et al*. Conduction slowing and sudden arrhythmic death in mice with cardiac-restricted inactivation of connexin43. *Circ Res* 2001;**88**:333–339.
6. Haberland M, Montgomery RL, Olson EN. The many roles of histone deacetylases in development and physiology: implications for disease and therapy. *Nat Rev Genet* 2009;**10**:32–42.
7. Colussi C, Mozzetta C, Gurtner A, Illi B, Rosati J, Straino S *et al*. HDAC2 blockade by nitric oxide and histone deacetylase inhibitors reveals a common target in Duchenne muscular dystrophy treatment. *Proc Natl Acad Sci USA* 2008;**105**:19183–19187.
8. Colussi C, Gurtner A, Rosati J, Illi B, Ragone G, Piaggio G *et al*. Nitric oxide deficiency determines global chromatin changes in Duchenne muscular dystrophy. *FASEB J* 2009;**23**:2131–2141.
9. Minetti GC, Colussi C, Adami R, Serra C, Mozzetta C, Parente V *et al*. Functional and morphological recovery of dystrophic muscles in mice treated with deacetylase inhibitors. *Nat Med* 2006;**12**:1147–1150.
10. Liu F, Levin MD, Petrenko NB, Lu MM, Wang T, Yuan LJ *et al*. Histone-deacetylase inhibition reverses atrial arrhythmia inducibility and fibrosis in cardiac hypertrophy independent of angiotensin. *J Mol Cell Cardiol* 2008;**45**:715–723.
11. Colussi C, Brioschi M, Tremoli E, Straino S, Spallotta F *et al*. Proteomic profile of differentially expressed plasma proteins from dystrophic mice and following suberoylanilide hydroxamic acid treatment. *Proteomics Clin Appl* 2010;**4**:71–83.
12. Sgoifo A, Stilli D, Medici D, Gallo P, Aimi B, Musso E. Electrode positioning for reliable telemetry ECG recordings during social stress in unrestrained rats. *Physiol Behav* 1996;**60**:1397–1401.
13. Kvetnansky R, Sun CL, Lake CR, Thoa N, Torda T, Kopin IJ. Effect of handling and forced immobilization on rat plasma levels of epinephrine, norepinephrine, and dopamine-beta-hydroxylase. *Endocrinology* 1978;**103**:1868–1874.
14. Peper K, Trautwein W. The effect of aconitine on the membrane current in cardiac muscle. *Pflugers Arch Gesamte Physiol Menschen Tiere* 1967;**296**:328–336.
15. Priori SG, Corr PB. Mechanisms underlying early and delayed afterdepolarizations induced by catecholamines. *Am J Physiol* 1990;**258**:H1796–H1805.
16. Kleber AG. The fibrillating atrial myocardium. What can the detection of wave breaks tell us? *Cardiovasc Res* 2000;**48**:181–184.
17. Smith JH, Green CR, Peters NS, Rothery S, Severs NJ. Altered patterns of gap junction distribution in ischemic heart disease. An immunohistochemical study of human myocardium using laser scanning confocal microscopy. *Am J Pathol* 1991;**139**:801–821.
18. Dupont E, Ko Y, Rothery S, Coppen SR, Baghai M, Haw M *et al*. The gap-junctional protein connexin40 is elevated in patients susceptible to postoperative atrial fibrillation. *Circulation* 2001;**103**:842–849.
19. Wang Y, Rudy Y. Action potential propagation in inhomogeneous cardiac tissue: safety factor considerations and ionic mechanism. *Am J Physiol Heart Circ Physiol* 2000;**278**:H1019–H1029.
20. Staub O, Abriel H, Plant P, Ishikawa T, Kanelis V, Saleki R *et al*. Regulation of the epithelial Na+ channel by Nedd4 and ubiquitination. *Kidney Int* 2000;**57**:809–815.
21. van Bemmelen MX, Rougier JS, Gavillet B, Apotheloz F, Daidie D, Tateyama M *et al*. Cardiac voltage-gated sodium channel Nav1.5 is regulated by Nedd4-2 mediated ubiquitination. *Circ Res* 2004;**95**:284–291.
22. Severs NJ. Gap junction remodeling in heart failure. *J Card Fail* 2002;**8**:S293–S299.
23. Sachse FB, Moreno AP, Seemann G, Abildskov JA. A model of electrical conduction in cardiac tissue including fibroblasts. *Ann Biomed Eng* 2009;**37**:874–889.
24. Abriel H. Cardiac sodium channel Nav1.5 and its associated proteins. *Arch Mal Coeur Vaiss* 2007;**100**:787–793.
25. Baba S, Dun W, Cabo C, Boyden PA. Remodeling in cells from different regions of the reentrant circuit during ventricular tachycardia. *Circulation* 2005;**112**:2386–2396.
26. Frank JS, Mottino G, Chen F, Peri V, Holland P, Tuana BS. Subcellular distribution of dystrophin in isolated adult and neonatal cardiac myocytes. *Am J Physiol* 1994;**267**:C1707–C1716.
27. Allouis M, Le Bouffant F, Wilders R, Peroz D, Schott JJ, Noireaud J *et al*. 14-3-3 is a regulator of the cardiac voltage-gated sodium channel Nav1.5. *Circ Res* 2006;**98**:1538–1546.
28. Mohler PJ, Rivolta I, Napolitano C, LeMaillet G, Lambert S, Priori SG *et al*. Nav1.5 E1053K mutation causing Brugada syndrome blocks binding to ankyrin-G and expression of Nav1.5 on the surface of cardiomyocytes. *Proc Natl Acad Sci USA* 2004;**101**:17533–17538.
29. Wu L, Yong SL, Fan C, Ni Y, Yoo S, Zhang T *et al*. Identification of a new co-factor, MOG1, required for the full function of cardiac sodium channel Nav 1.5. *J Biol Chem* 2008;**283**:6968–6978.